VTT Technical Research Centre of Finland

All-Wood Composite Material by Partial Fiber Surface Dissolution with an Ionic Liquid

Khakalo, Alexey; Tanaka, Atsushi; Korpela, Antti; Hauru, Lauri K.J.; Orelma, Hannes

Published in:
ACS Sustainable Chemistry & Engineering

DOI:
10.1021/acssuschemeng.8b05059

Published: 04/02/2019

Document Version
Publisher's final version

ACS Sustainable Chemistry & Engineering

Research Article

Cite This: ACS Sustainable Chem. Eng. 2019, 7, 3195−3202

pubs.acs.org/journal/ascecg

All-Wood Composite Material by Partial Fiber Surface Dissolution with an Ionic Liquid

Alexey Khakalo,[†] Atsushi Tanaka,[†] Antti Korpela,[†] Lauri K. J. Hauru,[‡] and Hannes Orelma*[,†]

[†]VTT - Technical Research Centre of Finland, Tietotie 4E, P.O. Box 1000, FI-02044 Espoo, Finland

[‡]University of Helsinki, P.O. Box 55 (A. I. Virtasen aukio 1), FI-00014, United States University of Helsinki

ABSTRACT: Synthetic structural materials of high mechanical performance are typically either of large weight (for example, steels, and alloys) or involve complex manufacturing processes and thus have high cost or cause adverse environmental impact (for example, polymer-based and biomimetic composites). In this perspective, low-cost, abundant and nature-based materials, such as wood, represent particular interest provided they fulfill the requirements for advanced engineering structures and applications, especially when manufactured totally additive-free. Here, we report on a novel all-wood material concept based on delignification, partial surface dissolution using ionic liquid (IL) followed by densification resulting in a high-performance material. A delignification process using sodium chlorite in acetate buffer solution was applied to controllably delignify the entire bulk wooden material while retaining the highly beneficial structural directionality of wood. In a subsequent step, obtained delignified porous wood template was infiltrated with an IL 1-ethyl-3-methylimidazolium acetate, [EMIM]OAc and heat activated at 95 °C to partially dissolve the fiber surface. Afterward, treated wood was washed with water to remove IL and hot-pressed to gain a very compact cellulosic material with fused fibers while retaining unidirectional fiber orientation. The obtained cellulose materials were structurally, chemically, and mechanically characterized revealing superior tensile properties compared to native wood. Furthermore, suggested approach allows almost 8-fold tensile strength improvement in the direction perpendicular to fiber orientation, which is otherwise very challenging to achieve.

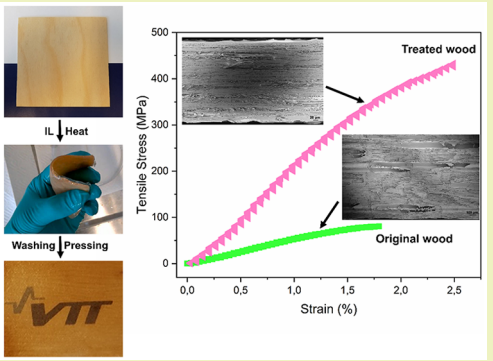

KEYWORDS: *All-cellulose composite, Ionic liquid, Dissolution, Delignification, Wood modification*

INTRODUCTION

Wood is the most widely used renewable biomaterial naturally synthesized by plants via photosynthesis. Its unique hierarchical microstructure and fibrous architecture with aligned fibers, composed of rigid cell walls that consist of high-strength cellulose fibrils embedded in a plant matrix of hemicelluloses and lignin, result in versatile features such as low density, high modulus, high strength, high toughness, and low thermal conductivity.[1,2] Therefore, this natural unique material has found many commercial applications from wood buildings to durable packages.

Recently, efforts have been devoted to modify the sophisticated wood structure in order to add novel specific functional properties to broaden the application area of wood. These include transparency,[3] electrical properties,[4−6] magnetism,[7,8] stimuli-responsiveness,[9] biosorption,[10] and oil−water separation features[11,12] as well as supercapacitance.[13] Nevertheless, it should be noted that all of these modifications still rely on utilization on synthetic polymers and thus detract significantly from the ecological benefits of using wood materials. Recently, a protocol involving delignification and subsequent densification steps was suggested for the transformation of wood into high-performance engineering materials.[14,15] Moreover, following same method, anisotropic, transparent films with aligned cellulose nanofibers could be fabricated directly from wood.[16]

Another alternative to fabricate next generation high-performance materials is an all-cellulose composite (ACC) approach, which utilizes cellulose for both the matrix and reinforcement. In such single-polymer composites, highly crystalline cellulose is used to reinforce a matrix of regenerated cellulose.[17−19] As a result, materials with extremely high mechanical properties can be produced due to strong interfacial adhesion within the components. All-cellulose composites are fabricated either (1) from completely dissolved cellulose combined with undissolved cellulose and subsequent regeneration to form the matrix phase or (2) by partial dissolution of the cellulose surface followed by regeneration to form a matrix phase.

A large variety of the suitable nonderivatizing and derivatizing dissolution systems have been reported for cellulose. Nonderivatizing direct dissolution chemistries such as cupro, NMMO·H_2O, lithium chloride/*N*,*N*-dimethylacetamide (LiCl/DMAc) and ionic liquids (ILs) are attractive since

Received: October 2, 2018
Revised: December 5, 2018
Published: January 8, 2019

Scheme 1. Schematic Illustration of the All-Wood Composite Fabrication Process

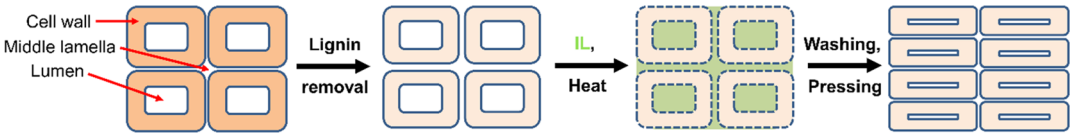

they do not alter the chemistry of cellulose, maintaining its excellent biodegradability.[20,21] It is also important to mention that the choice of cellulose solvent is crucial as it will determine the "greenness" of the final material. So-called "green solvents" should (1) be nontoxic and easily biodegradable, thereby providing safe work conditions, (2) be efficiently recycled in order to avoid their propagation in ecosystems, and (3) have a low energy production cycle. In this context, ILs are promising solvents that address all of the three above-mentioned environmental points. Moreover, ILs can be used to prepare new all-lignocellulosic materials as they are able to dissolve cellulose, hemicellulose and in part, lignin and wood.[22] For example, partial dissolution with 1-butyl-3-methylimidazolium chloride ([BMIM]Cl) has been utilized to produce an all-wood composite from hinoki wood.[23] The wood specimen was dipped into a liquid of [BMIM[Cl at 100 °C for 30 min followed by hot-pressing. This resulted in tensile modulus improvement only, whereas tensile strength and elongation at break deteriorated compared to untreated wood. Mechanical properties comparable to injection molded high density polyethylene or neat polypropylene were achieved for lignocellulosic composites prepared by partially dissolving cotton along with steam exploded aspen wood and burlap fabric reinforcements utilizing an IL ([EMIM]OAc).[24] Same IL has been shown to completely dissolve both softwood and hardwood.[25] Moreover, [EMIM]OAc has desirable properties such as low toxicity (LD_{50} > 2000 mg kg^{-1}), low corrosiveness, low melting point (<−20 °C), low viscosity (~140 mPas at 25 °C and 10 mPa s at 80 °C), and favorable biodegradability.[26]

Recently, we have demonstrated the "'chemical welding"' of paper with [EMIM]OAc resulting in an all-cellulose material with improved both dry and wet strength.[27] In this contribution, we present a simple method to fabricate all-wood composites while retaining the beneficial hierarchical structure and fiber directionality of wood, Scheme 1. For this, delignified wood template was impregnated with ionic liquid 1-ethyl-3-methylimidazolium acetate ([EMIM]OAc), followed by heat activation in an oven to partially dissolve the fiber surface. Afterward, the IL was removed from wood by washing with water and, finally, the wood samples were pressed while heated. The obtained all-wood material was structurally, chemically, and mechanically characterized.

EXPERIMENTAL SECTION

Wood Delignification. Birch wood plies (Metsä Wood) with a thickness of 1.5 ± 0.1 mm and a density of 530 kg/m^3 were cut to the dimensions of 10 × 10 cm and stored at 23 °C and 50% relative humidity (RH). Wood samples (130 g dry weight) were treated under stirring using 1 wt % sodium chlorite ($NaClO_2$, Sigma-Aldrich) in acetate buffer solution (3000 mL, pH 4.6) at 80 °C for 12 h.[28] This treatment was repeated 2 times with rinsing the samples with Milli-Q water for 1 h between the extraction steps. The delignified samples were carefully washed with Milli-Q water overnight followed by drum drying between blotting papers for 6 h at 60 °C. Afterward, delignified wood samples were conditioned at 23 °C and 50% RH.

All-Wood Material Preparation. Wood modification employed partial dissolution of cellulose fibers followed by their fusion under pressure. First, the delignified wood template (moisture content of 8.6%) was infiltrated by ionic liquid (IL) 1-ethyl-3-methylimidazolium acetate, [EMIM]OAc, (>95% purity, purchased from IoLiTec Ionic Liquids Technologies GmbH, Germany) under vacuum (≤15 mbar) for 30 min. Vacuum infiltration was repeated three times to ensure the full wood infiltration. After slight draining to remove excess of IL, infiltrated wood was placed on a metal plate and heat activated in an oven at 95 °C for 30 min. Next, heat activated samples were washed with Milli-Q-purified water to remove IL. Water was replaced every hour for 4 consecutive hours at room temperature until washing water became colorless. Washed samples were then covered with Sefar PETEX 07−1/2 monofilament open mesh fabrics and blotting papers. Finally, they were dried with a hot press between stainless steel sheets under 5 MPa for 16 h at 100 °C. Dried samples were stored at 23 °C and 50% RH. Original, nondelignified wood (OW) was subjected to the same procedure and was used as a reference.

Fast Heat Activation Using Hot Calender. Heat activation of IL-impregnated wood, in addition to the treatment in an oven, was also carried out with a self-made hot calender, Figure 5a. The calender consisted of two rolls: an upper heated smooth steel roll equipped with the surface temperature control and a lower rubber-coated roll. The IL-impregnated wood was passed through the nip between these rolls at a temperature of 130 °C, speed of 1 m/min, and a line load of approximately 30 kN/m. The surface temperature of the sample was monitored with a portable infrared thermometer. More details regarding this procedure could be found in Orelma et al.[29] Afterward, the sample was removed from the metal roll with a sharp blade and placed in water to remove IL following the same procedure as described above.

Sample Characterizations. *SEM Investigation.* The surface and cross section of delignified wood and all-wood composite materials were observed with a Merlin FE-SEM (Carl Zeiss NTS GmbH, Germany). The imaging was performed using the 1.5 keV electron energy using both secondary electron and InLens detectors. The cross section of the samples was prepared using Leica RM2255 rotation microtome. All samples were gold sputter coating at 20 mA for 30 s before SEM characterization. The image pixel resolution was 2048 × 1536.

Carbohydrate and Lignin Composition. To determine the carbohydrate and lignin composition, the samples were hydrolyzed with sulfuric acid (2 stages) and the resulting monosaccharides were determined by HPAEC with pulse amperometric detection (Dionex ICS 5000 equipped with CarboPac PA20 column).[30] The acid-insoluble lignin content (Klason lignin) in wood samples was determined according to TAPPI method (TAPPI T 222 om-02). The acid-soluble lignin was determined by a spectrophotometric method based on absorption of ultraviolet radiation at 215 and 280 nm using equation described by Goldschmid.[31] Nitrogen content was determined using a FLASH 2000 series analyzer.[32] three replicates of each sample type were measured and the average values are reported.

Chemistry by FTIR-ATR. The chemical changes of wood due to delignification as well as partial dissolution were investigated with a Thermo Scientific Nicolet iS50 FTIR spectrometer with an ATR diamond (Thermo Scientific). All spectra were obtained from 32 scans with a resolution of 4 cm^{-1} and absorption mode by using the wavelength range from 400 to 4000 cm^{-1}.

Crystallinity by Solid State NMR. The changes in the crystallinity of the wood after delignification process and partial dissolution with IL were investigated with a ^{13}C cross-polarization magic angle spinning (CP MAS) NMR spectrometer (Bruker AVANCE-III 400 MHz, Bruker BioSpin, Germany). For all samples, 20 000 scans were

DOI: 10.1021/acssuschemeng.8b05059
ACS Sustainable Chem. Eng. 2019, 7, 3195−3202

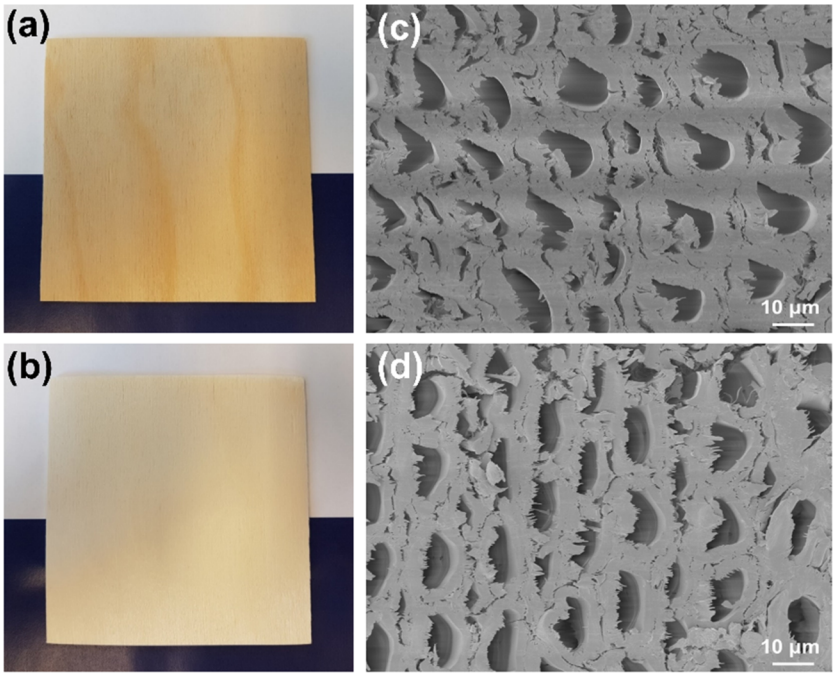

Figure 1. Delignification of wood: an optical image of original wood (OW) before (a) and after (b) delignification (DLW). Cross section images of original wood (c) showing the micro structure of wood and delignified wood (d) supporting the presence of a well-preserved wood structure after delignification.

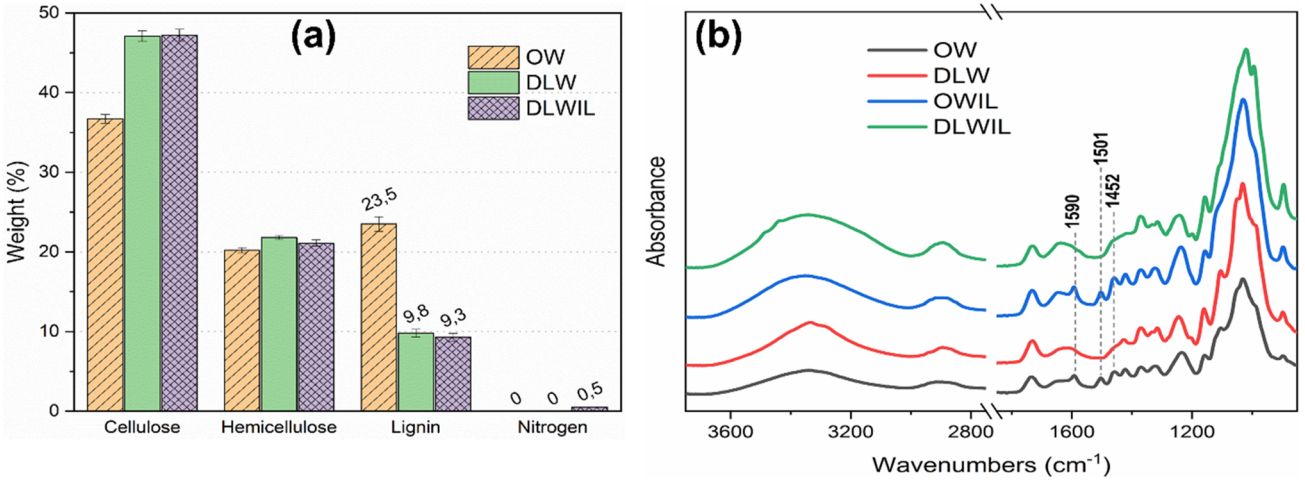

Figure 2. Chemical treatment leads to substantial removal of lignin (from 23.5% ± 0.9 to 9.8% ± 0.5%) (a). ATR-FTIR spectra of fabricated wood samples in the spectral range from 3800 to 900 cm^{-1} (b). OW and DLW denote original and delignified wood samples, respectively and OWIL and DLWIL denote original and delignified wood samples treated with ionic liquid (IL), respectively.

collected using 8 kHz spinning frequency, 2 ms contact time and 5 s delay between pulses.

Porosity of Samples by BET. The Brunauer–Emmett–Teller (BET) nitrogen absorption was carried out with a Micromeritics 3Flex Physiosorpio instrument (Micromeritics Instrument Corp. Norcross, GA). Specimen size was approximately 0.5 × 0.5 cm^2. The specimens were put into a measurement tubes and dehydrated in a VacPrep 061 vacuum device at 125 °C for 7–14 h. Then the absorption isotherms of water free specimens were measured with nitrogen gas at temperature of liquid nitrogen. Specific surface areas of the specimens were calculated from the measured adsorption isotherms by using the BET theory. Two replicates of each sample type were measured and the average values are reported.

Mechanical Performance. Mechanical properties of prepared samples were measured at 10%/min strain rate and 25 mm of span using a MTS 400/M (MTS Systems, USA) vertical tensile tester with a load cell of 1 kN equipped with TestWorks 4.02 measuring program. All samples were conditioned for at least 24 h at 50% relative humidity and a temperature of 23 °C. Each sample was cut into a strip (5 × 50 mm) for testing. At least five replicates of each sample type were measured and the average values are reported.

Optical Properties. Diffusive transmittance of all-wood composites was measured involving an integrating sphere with a Cary 5000 UV–vis-NIR Spectrophotometer (Agilent Technologies) between 800 and 300 nm at a scan rate of 600 nm/min, data interval 1 nm.

RESULTS AND DISCUSSION

Delignification and Characterization. The wood cell wall is composed of more than 50% of matrix substances such as lignin and hemicellulose that are interconnected with microfibrils.[33] Mechanical properties of these matrix sub-

DOI: 10.1021/acssuschemeng.8b05059
ACS Sustainable Chem. Eng. 2019, 7, 3195–3202

stances are not as high as for microfibrils. Moreover, lignin fills the voids and is distributed on the surface of hemicelluloses covered cellulose fibers. Thus, in a first step, lignin was partially removed by chemical extraction of wood with sodium chlorite to increase the inner pore size and as a result the swelling of the fibers. Figure 1a,b shows the appearance of wood before and after delignification. Lignin is originally of brownish color due to its phenolic character.[34] As a result, due to partial removal of lignin, a cellulose-rich scaffold of white color is attained while the orientation of the cellulose microfibrils as well as the shape of wood are preserved. Chemical treatment leads to reduction of lignin content in natural wood from 23.5 to 9.8%, Figure 2a. It is worth noting that increasing the delignification time makes it impossible to keep the wood integrity leading to fibers/wood structure disintegration. Lignin removal is also evident from the absence of characteristic lignin peaks at 1590/1501 cm^{-1} (C=C stretching vibration) and 1452 cm^{-1} (asymmetric bending in CH_3), which are attributed to the aromatic skeletal vibrations, Figure 2b. Despite lignin removal, the honeycomb-like structure and cell wall organization of wood are well-preserved, Figure 1c,d. Nevertheless, BET surface area measurements indicate almost 4-fold decrease in porosity of delignified wood compared to that of original wood, Figure 3d. This could be attributed to the hornification type of effect, as partial lignin removal tends to facilitate wood shrinking during drying causing collapsing of some of the pores in the wood structure. This could be avoided by implementing drying techniques like freeze-drying or solvent exchange; however, they cannot be realized at industrial scale at low costs.

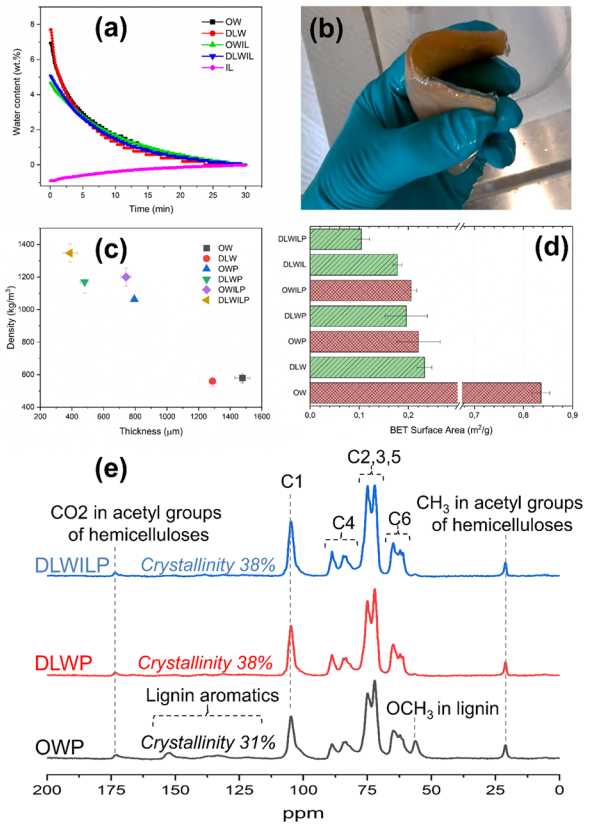

Figure 3. Evaporation of the water from wood samples as a function of heating time at 95 °C (a), photo of flexible gel-type wood after washing with water to remove ionic liquid (b), density and thickness (c), BET surface area (d), and ^{13}C CP/MAS NMR spectra of wood samples. OW and DLW denote original wood and delignified wood, respectively, OWP and DLWP denote original wood and delignified wood after pressing, respectively, and OWILP and DLWILP denote original wood and delignified wood after ionic liquid treatment and pressing, respectively.

All-Wood Composite Fabrication. After partial lignin removal, the cellulose-based scaffold was vacuum-impregnated with the ionic liquid (IL) 1-ethyl-3-methylimidazolium acetate, [EMIM]OAc. The samples were weighed before and after IL impregnation to assess the wood:IL ratio, which was 1:1 based on dry weight almost for all samples after removing excess of IL. Next, IL-impregnated wood samples were activated in an oven at 95 °C for 30 min. Figure 3a reveals that IL-impregnated wood loses most of the moisture within the selected activation time of 30 min. For comparison, original, and delignified wood were subjected to the same analysis. Interestingly, samples that were not infiltrated with IL had higher initial water contact level but after 5 min the water content was identical for all samples. This indicates that during the vacuum-facilitated IL infiltration some of the moisture was evaporated due to low pressure (≤15 mbar) utilized for this purpose as all the samples were conditioned at 50% relative humidity beforehand. Moreover, delignified wood had higher initial water content than original wood due to lower amount of lignin present in the cell wall, which is known for its hydrophobic nature. After water is evaporated, IL-facilitated wood dissolution is believed to become more effective even though [EMIM]OAc is a special case among ionic liquids because it can tolerate water: it has been shown that microcrystalline cellulose (MCC) can be dissolved at water contents as high as 15 wt %.[35] Water tolerance is desirable for a cellulose solvent, because water can be difficult to completely remove from cellulose-based materials due to the hydrophilic nature of cellulose.

In this study, heat treatment was kept short enough to prevent complete wood dissolution. As indicated in Figure 2a, amounts of cellulose and hemicellulose in delignified wood after IL treatment remained the same whereas lignin content slightly decreased (from 9.8 to 9.3 wt %). It could be hypothesized that low molecular fractions of lignin created during delignification step were further dissolved and removed during IL treatment and subsequent washing step, respectively. It is also worth noting that IL-treated samples showed traces of nitrogen, Figure 2a, despite the fact that ATR-FTIR measurements do not reveal peaks attributed to the C=N vibrations observed at 1565 cm^{-1}.[36] The penetration depth for ATR-FTIR experiment is estimated to be no more than about few microns into the surface[37] indicating that imidazole moieties are located in the bulk of the samples. It is likely that the side reaction occurs: a carbene is formed from the imidazolium, which then reacts with reducing end of cellulose to form a carbon−carbon bond.[38]

Subsequently, IL was removed by washing the samples with deionized water, which resulted in a flexible gel-type wood, Figure 3b. During heat activation, surface of cellulose fibers was first partially dissolved and then consequently regenerated into a gel-type layer leaving inner fiber structure intact. Figure 3b illustrates that the material's flexibility might allow facile designing of an objects with different shapes and complex geometries to be produced that fully maintain fiber alignment.

In a subsequent step, the wood bulk material was pressed while simultaneously heated. That increased the density from

DOI: 10.1021/acssuschemeng.8b05059
ACS Sustainable Chem. Eng. 2019, 7, 3195−3202

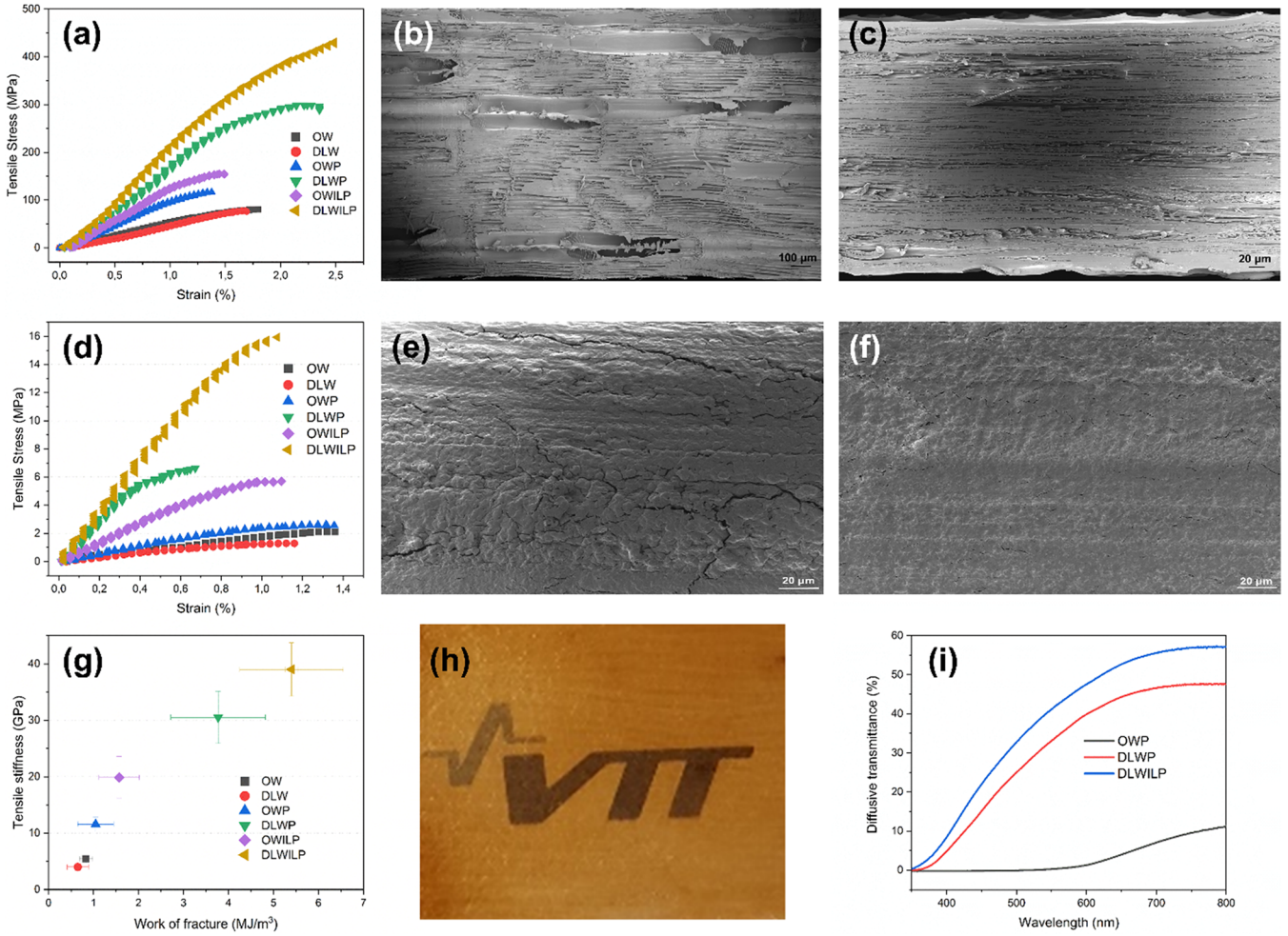

Figure 4. Stress−strain curves of wood samples in a direction along (longitudinal) (a) and perpendicular (transverse) to fiber orientation (d). SEM image of the original wood revealing the cross-section view of the lumen along the longitudinal direction (b). SEM image of the delignified, IL-treated and pressed wood in the longitudinal direction indicating full collapse of the lumen (c). SEM cross section images of delignified and pressed wood without (e) and with (f) ionic liquid treatment in the direction perpendicular to fiber orientation. Comparison of tensile stiffness and work of fracture (g) of different wood samples, error bars represent the standard deviation from at least five replicates. The optical image of ∼0.4 mm thick translucent delignified wood sample after IL treatment and pressing with size of 50 × 50 mm on substrate with VTT logo (h). Diffusive transmittance of pressed wood samples (i). The logo is used with permission from VTT. OW and DLW denote original wood and delignified wood, respectively, OWP and DLWP denote original wood and delignified wood after pressing, respectively, and OWILP and DLWILP denote original wood and delignified wood after ionic liquid treatment and pressing, respectively.

580 to 1063 kg/m^3 and from 560 to 1170 kg/m^3 for original and delignified wood, respectively. The delignification process facilitated cell collapse during pressing, most probably due to reduction of the transverse rigidity of the cell walls. As a result, the open spaces between the cell walls in original wood are eliminated leading to a unique laminated structure with cell walls tightly interconnected with each other. Upon IL treatment, a more pronounced cell folding of the cells could be observed and highly consolidated material with density of 1347 kg/m^3 was obtained after simultaneous pressing and heating (drying) of delignified wood, Figure 3c. Interestingly, density of original wood after IL treatment reached 1200 kg/m^3 whereas a value of 1063 kg/m^3 was found for pressed original wood.

Density is one of the dominating factors controlling mechanical properties of a material. Stress−strain curves presented in Figure 4a demonstrate the profound impact of the densification and IL treatment on the mechanical behavior of the fabricated wood samples. A comparison of the tensile strength and stiffness of the samples indicated that compression after IL treatment resulted in raised values and hence superior properties were achieved. For example, tensile strength of original wood increased from ≈80 to ≈115 and ≈155 MPa due to densification without and with IL treatment, respectively. A very similar trend was obtained for the tensile stiffness, again showing that densification after IL treatment is superior to the one without IL treatment, Figure 4g. Remarkably, in comparison with the original wood, the application of the same fabrication protocol for the delignified wood resulted in even more pronounced increase in tensile strength: from ≈75 up to ≈300 and ≈430 MPa due to densification without and with IL treatment, respectively. Moreover, the comparison in Figure 4g shows that the applied protocols allow for producing cellulose bulk materials, which are not only stiffer and stronger than original wood but also have a higher work of fracture. Despite moderate increase in strain to fracture for all tested samples, the specimens that were delignified, IL-treated and densified show superior properties

DOI: 10.1021/acssuschemeng.8b05059
ACS Sustainable Chem. Eng. 2019, 7, 3195−3202

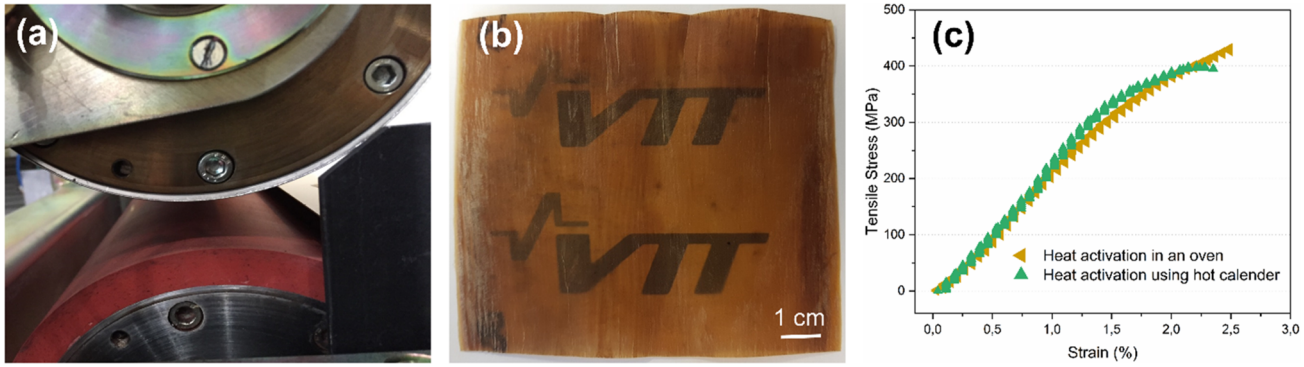

Figure 5. Photo of the nip of the hot calender utilized in the fast heat activation of the IL-impregnated delignified wood (a). The optical image of ~0.5 mm thick translucent delignified wood sample after IL treatment and heat activation in the calender with size of 10 × 10 cm on substrate with VTT logo (b). Stress−strain curves of delignified wood samples after IL treatment with different heat activation methods (c). The logo is used with permission from VTT.

for all mechanical parameters. A beneficial combination of stiffness, strength and toughness is crucial for many applications.

These results indicate the crucial importance of the delignification step for favoring the mechanical properties improvement. It is likely that the presence of lignin, located at the fiber surface, limits the exposure of the cellulose-rich area to chemical modifications. It has been shown earlier that the IL penetrates and solubilizes the outer surface of individual fibers, swells and opens the polymer structure, cellulose I is decrystallized, and hydrogen bonding networks are extended between adjacent fibers.[19] Therefore, the chemical properties in the modified wood samples were investigated with the FTIR-ATR spectroscopy (Figure 2b). Data curves OW and DLW are typical for the native wood containing primarily cellulose I. In particular, absorbance due to C−O stretching, C−O−C asymmetric stretching, COH and CCH deformation vibrations, and CH_2 wagging are observed at 1000−1300 cm^{-1} as well as O−H stretching at 2600−3500 cm^{-1}.[39,40] Spectra for IL-treated samples (OWIL and DLWIL), which are free of residual [EMIM]OAc, show changes in regions associated with hydrogen bonding and crystallinity. To be more specific, characteristic cellulose I peaks at these regions lose definition (peak shifts of the bands at 1022−1015 and 895−990 cm^{-1}, corresponding to the CO stretching vibrations at C_6 position of the anhydropyranose occurred) and broaden (O−H stretching at 2600−3500 cm^{-1}) as crystallinity is lost when cellulose I is converted to cellulose II. The changes in the cellulose crystallinity of the IL-treated wood were also investigated with a solid state ^{13}C CP MAS NMR spectrometer, Figure 3e. In contrast to the FTIR-ATR observations, the typical peaks of regenerated cellulose after IL dissolution did not appear in the NMR signal[41] and the carbon signal of the wood did not change significantly.[42] The discrepancy in these observations is most likely due to the fact that the FTIR-ATR analysis probes the outer surface properties (1 to 4 μm)[37] while NMR is a bulk analysis technique. Therefore, it can be concluded that chemical modifications due to IL treatment primary took place at the surface of cellulose fibers leaving inside structure intact. It is also worth noting, that mechanical properties in the direction perpendicular to fiber orientation were also improved. Remarkably, IL-treated delignified sample was almost 2.5 times stronger (≈16 MPa vs ≈6.6 MPa) when compared to delignified sample after pressing and about 8 times stronger (≈16 MPa vs ≈2 MPa) when compared to original wood. This indicates that regenerated jelly layer most likely promotes better interconnection between fibers during pressing. As evident from Figures 4e,f, IL-treated delignified cells were uniformly compressed and almost no cracks could be observed in the cell walls, whereas densified delignified bulk wood showed extensive cell wall cracking. This explains the superior mechanical properties of IL-treated samples as in this case uniform stress transfer upon loading is observed. Overall, tensile tests of the fabricated wood show that remarkable material properties improvements can be achieved. Moreover, it is important to emphasize here that the tested samples were entirely composed of wood components (totally additive-free) and therefore only the bonding forces between the aligned cells and cellulose fibrils were decisive.

Besides the improved mechanical performance, the fabricated material has certain degree of transparency that could benefit different applications (Figure 4h). According to Snell's law, light is diffracted as it passes through an interface,[43] for example, the larger the difference in refractive indices between the two media, the larger the diffraction angle will be. In wood, light scattering takes place at the interface between the cell wall (refractive index ≈1.53 based on cellulose and hemicellulose) and air (refractive index 1.0) in the lumen and between cellulose nanofibers and air in the cell wall. BET porosity of original and delignified wood after pressing was practically identical: 0.22 and 0.20 m^2/g, respectively. However, light transmittance of original wood is much lower due to lignin presence, which is a strong light absorbent biopolymer that accounts for 80−95% of the light absorption.[44] As high diffusive transmittance as 48% at 600 nm (or 42% at 550 nm) was achieved for delignified, IL-treated and pressed sample as a result of low porosity (0.10 m^2/g) indicating that IL treatment facilitated interface removal within the fabricated sample.

Fast Heat Activation Using Hot Calender. Implementation of fast heat activation step of the IL-impregnated delignified wood resulted in a material with certain degree of transparency (Figure 5b) and with similar mechanical properties as when activation in an oven is performed, Figure 5c. That allows dramatical time saving needed for the all-wood composite preparation (30 min in an oven compared to few seconds using the hot calendar). Furthermore, varying the pressure between the rolls might bring another benefits like (1) better material consolidation due to IL-facilitated H-bonding disruption between wood polymers thus better contact

DOI: 10.1021/acssuschemeng.8b05059
ACS Sustainable Chem. Eng. 2019, 7, 3195−3202

between the fibers could be achieved when pressure is applied. (2) Water washing step required to remove the IL might be significantly shortened as most of the IL is effectively squeezed from the wood.

CONCLUSIONS

An all-wood composite material was fabricated in a stepwise process of delignification, IL-facilitated partial fiber surface dissolution and subsequent heat-assisted densification. This allowed embedding the still undissolved parts of fibers into a matrix of regenerated cellulose, which resulted in compact composites with an extraordinary mechanical performance. For the delignified, IL-treated and pressed samples, an average tensile stiffness of ∼39 GPa and a tensile strength of ∼430 MPa were reached. This is accompanied by an improved work of fracture (5.4 MJ/m^3) compared to unmodified wood (0.8 MJ/m^3), which in combination with the high stiffness, is highly desired. Moreover, almost 8-fold tensile strength improvement in the direction perpendicular to fiber orientation was achieved. Overall, even without adding any matrix system, the obtained mechanical properties were superior to wood and many other natural fiber-reinforced composites. On the basis of the observations presented here, the future work could be extended toward preparation of various 3D-shaped structures with highly aligned fibers, which will add value to the future circular bioeconomy.

AUTHOR INFORMATION

Corresponding Author

*Phone: +358403543143; e-mail: hannes.orelma@vtt.fi.

ORCID

Hannes Orelma: 0000-0001-5070-9542

Author Contributions

The manuscript was written through contributions of all authors. All authors have given approval to the final version of the manuscript.

Notes

The authors declare no competing financial interest.

ACKNOWLEDGMENTS

This study was carried out in the CellFi (Conversion of cellulose to plastic) project funded by Business Finland and Finnish industrial companies (Metsä Fibre Ltd, Metsä Board Ltd, Stora Enso Ltd, FL Pipe Ltd, Pölkky Ltd and Versoul Ltd). Kimmo Velling is thanked for carrying out the cross section preparations for SEM imaging, Atte Mikkelson is acknowledged for carbohydrate and lignin determinations, Tommi Virtanen and Mirja Muhola are thanked for performing the NMR and BET analyses, respectively. Professor Ilkka Kilpeläinen (University of Helsinki) is thanked for active participation in the CellFi project. The work was part of the Academy of Finland Flagship Programme under Project Nos. 318890 and 318891 (Competence Center for Materials Bioeconomy, FinnCERES).

REFERENCES

(1) Vay, O.; De Borst, K.; Hansmann, C.; Teischinger, A.; Müller, U. Thermal Conductivity of Wood at Angles to the Principal Anatomical Directions. *Wood Sci. Technol.* **2015**, *49*, 577−589.

(2) Cabane, E.; Keplinger, T.; Künniger, T.; Merk, V.; Burgert, I. Functional Lignocellulosic Materials Prepared by ATRP from a Wood Scaffold. *Sci. Rep.* **2016**, *6*, 31287.

(3) Li, Y.; Fu, Q.; Yu, S.; Yan, M.; Berglund, L. Optically Transparent Wood from a Nanoporous Cellulosic Template: Combining Functional and Structural Performance. *Biomacromolecules* **2016**, *17*, 1358−1364.

(4) Wan, J.; Song, J.; Yang, Z.; Kirsch, D.; Jia, C.; Xu, R.; Dai, J.; Zhu, M.; Xu, L.; Chen, C.; et al. Highly Anisotropic Conductors. *Adv. Mater.* **2017**, *29*, 1703331.

(5) Chen, C.; Zhang, Y.; Li, Y.; Dai, J.; Song, J.; Yao, Y.; Gong, Y.; Kierzewski, I.; Xie, J.; Hu, L. All-Wood, Low Tortuosity, Aqueous, Biodegradable Supercapacitors with Ultra-High Capacitance. *Energy Environ. Sci.* **2017**, *10*, 538−545.

(6) Chen, C.; Li, Y.; Song, J.; Yang, Z.; Kuang, Y.; Hitz, E.; Jia, C.; Gong, A.; Jiang, F.; Zhu, J. Y.; et al. Highly Flexible and Efficient Solar Steam Generation Device. *Adv. Mater.* **2017**, *29*, 1701756.

(7) Merk, V.; Chanana, M.; Gierlinger, N.; Hirt, A. M.; Burgert, I. Hybrid Wood Materials with Magnetic Anisotropy Dictated by the Hierarchical Cell Structure. *ACS Appl. Mater. Interfaces* **2014**, *6*, 9760−9767.

(8) Trey, S.; Olsson, R. T.; Ström, V.; Berglund, L.; Johansson, M. Controlled Deposition of Magnetic Particles within the 3-D Template of Wood: Making Use of the Natural Hierarchical Structure of Wood. *RSC Adv.* **2014**, *4*, 35678−35685.

(9) Keplinger, T.; Cabane, E.; Berg, J. K.; Segmehl, J. S.; Bock, P.; Burgert, I. Smart Hierarchical Bio-Based Materials by Formation of Stimuli-Responsive Hydrogels inside the Microporous Structure of Wood. *Adv. Mater. Interfaces* **2016**, *3*, 1600233.

(10) Vitas, S.; Keplinger, T.; Reichholf, N.; Figi, R.; Cabane, E. Functional Lignocellulosic Material for the Remediation of Copper-(II) Ions from Water: Towards the Design of a Wood Filter. *J. Hazard. Mater.* **2018**, *355*, 119−127.

(11) Chen, F.; Gong, A. S.; Zhu, M.; Chen, G.; Lacey, S. D.; Jiang, F.; Li, Y.; Wang, Y.; Dai, J.; Yao, Y.; et al. Mesoporous, Three-Dimensional Wood Membrane Decorated with Nanoparticles for Highly Efficient Water Treatment. *ACS Nano* **2017**, *11*, 4275−4282.

(12) del Blanco, M.; Fischer, E. J.; Cabane, E. Underwater Superoleophobic Wood Cross Sections for Efficient Oil/Water Separation. *Adv. Mater. Interfaces* **2017**, *4*, 1700584.

(13) Lyu, S.; Chen, Y.; Han, S.; Guo, L.; Yang, N.; Wang, S. Natural Sliced Wood Veneer as a Universal Porous Lightweight Substrate for Supercapacitor Electrode Materials. *RSC Adv.* **2017**, *7*, 54806−54812.

(14) Frey, M.; Widner, D.; Segmehl, J. S.; Casdorff, K.; Keplinger, T.; Burgert, I. Delignified and Densified Cellulose Bulk Materials with Excellent Tensile Properties for Sustainable Engineering. *ACS Appl. Mater. Interfaces* **2018**, *10*, 5030−5037.

(15) Song, J.; Chen, C.; Zhu, S.; Zhu, M.; Dai, J.; Ray, U.; Li, Y.; Kuang, Y.; Li, Y.; Quispe, N.; et al. Processing Bulk Natural Wood into a High-Performance Structural Material. *Nature* **2018**, *554*, 224−228.

(16) Zhu, M.; Wang, Y.; Zhu, S.; Xu, L.; Jia, C.; Dai, J.; Song, J.; Yao, Y.; Wang, Y.; Li, Y.; et al. Anisotropic, Transparent Films with Aligned Cellulose Nanofibers. *Adv. Mater.* **2017**, *29*, 1606284.

(17) Nishino, T.; Matsuda, I.; Hirao, K. All-Cellulose Composite. *Macromolecules* **2004**, *37*, 7683−7687.

(18) Gindl, W.; Keckes, J. All-Cellulose Nanocomposite. *Polymer* **2005**, *46*, 10221−10225.

(19) Haverhals, L. M., Foley, M. P., Brown, E. K., Fox, D. M., De Long, H. C.; Trulove, P. C. Natural fiber welding: Ionic liquid facilitated biopolymer mobilization and reorganization. In *Ionic Liquids: Science and Applications*, 2012; pp 145−166.

(20) Liebert, T. Cellulose solvents—remarkable history, bright future. In *Cellulose Solvents: For Analysis, Shaping and Chemical Modification*; Liebert, T., Ed.; American Chemical Society, Washington, DC, 2010; pp 1−3.

(21) Eichhorn, S. J.; Dufresne, A.; Aranguren, M.; Marcovich, N. E.; Capadona, J. R.; Rowan, S. J.; Weder, C.; Thielemans, W.; Roman, M.; Renneckar, S.; et al. Review: Current International Research into Cellulose Nanofibres and Nanocomposites. *J. Mater. Sci.* **2010**, *45*, 1−33.

DOI: 10.1021/acssuschemeng.8b05059
ACS Sustainable Chem. Eng. 2019, 7, 3195−3202

(22) Brandt, A.; Gräsvik, J.; Hallett, J. P.; Welton, T. Deconstruction of Lignocellulosic Biomass with Ionic Liquids. *Green Chem.* **2013**, *15*, 550−583.
(23) Shibata, M.; Teramoto, N.; Nakamura, T.; Saitoh, Y. All-Cellulose and All-Wood Composites by Partial Dissolution of Cotton Fabric and Wood in Ionic Liquid. *Carbohydr. Polym.* **2013**, *98*, 1532−1539.
(24) Tisserat, B.; Larson, E.; Gray, D.; Dexter, N.; Meunier, C.; Moore, L.; Haverhals, L. Ionic Liquid-Facilitated Preparation of Lignocellulosic Composites. *Int. J. Polym. Sci.* **2015**, *2015*, 181097.
(25) Sun, N.; Rahman, M.; Qin, Y.; Maxim, M. L.; Rodríguez, H.; Rogers, R. D. Complete Dissolution and Partial Delignification of Wood in the Ionic Liquid 1-Ethyl-3-Methylimidazolium Acetate. *Green Chem.* **2009**, *11*, 646−655.
(26) Cao, Y.; Wu, J.; Zhang, J.; Li, H.; Zhang, Y.; He, J. Room Temperature Ionic Liquids (RTILs): A New and Versatile Platform for Cellulose Processing and Derivatization. *Chem. Eng. J.* **2009**, *147*, 13−21.
(27) Tanaka, A.; Khakalo, A.; Hauru, L.; Korpela, A.; Orelma, H. Conversion of Paper to Film by Ionic Liquids: Manufacturing Process and Properties. *Cellulose* **2018**, *25*, 6107−6119.
(28) Yano, H.; Hirose, A.; Collins, P. J.; Yazaki, Y. Effects of the Removal of Matrix Substances as a Pretreatment in the Production of High Strength Resin Impregnated Wood Based Materials. *J. Mater. Sci. Lett.* **2001**, *20*, 1125−1126.
(29) Orelma, H.; Korpela, A.; Kunnari, V.; Harlin, A.; Suurnäkki, A. Improving the Mechanical Properties of CNF Films by NMMO Partial Dissolution with Hot Calender Activation. *Cellulose* **2017**, *24*, 1691−1704.
(30) Willför, S.; Pranovich, A.; Tamminen, T.; Puls, J.; Laine, C.; Suurnäkki, A.; Saake, B.; Uotila, K.; Simolin, H.; Hemming, J.; et al. Carbohydrate Analysis of Plant Materials with Uronic Acid-Containing Polysaccharides−A Comparison between Different Hydrolysis and Subsequent Chromatographic Analytical Techniques. *Ind. Crops Prod.* **2009**, *29*, 571−580.
(31) Goldschmid, O. Ultraviolet Spectra. In *Lignins: Occurrence, Formation, Structure and Reactions*; Sarkanen, K. V., Ludwig, C. H., Eds.; John Wiley & Sons, New York, 1971; pp 241−298.
(32) Nordlund, E.; Lille, M.; Silventoinen, P.; Nygren, H.; Seppänen-Laakso, T.; Mikkelson, A.; Aura, A. M.; Heiniö, R. L.; Nohynek, L.; Puupponen-Pimiä, R.; et al. Plant Cells as Food − A Concept Taking Shape. *Food Res. Int.* **2018**, *107*, 297−305.
(33) Sarkar, P.; Bosneaga, E.; Auer, M. Plant Cell Walls throughout Evolution: Towards a Molecular Understanding of Their Design Principles. *J. Exp. Bot.* **2009**, *60*, 3615−35.
(34) Wang, J.; Deng, Y.; Qian, Y.; Qiu, X.; Ren, Y.; Yang, D. Reduction of Lignin Color via One-Step UV Irradiation. *Green Chem.* **2016**, *18*, 695−699.
(35) Tan, X.; Li, X.; Chen, L.; Xie, F. Solubility of Starch and Microcrystalline Cellulose in 1-Ethyl-3-Methylimidazolium Acetate Ionic Liquid and Solution Rheological Properties. *Phys. Chem. Chem. Phys.* **2016**, *18*, 27584−27593.
(36) FitzPatrick, M.; Champagne, P.; Cunningham, M. F. Quantitative Determination of Cellulose Dissolved in 1-Ethyl-3-Methylimidazolium Acetate Using Partial Least Squares Regression on FTIR Spectra. *Carbohydr. Polym.* **2012**, *87*, 1124−1130.
(37) Haverhals, L. M.; Sulpizio, H. M.; Fayos, Z. A.; Trulove, M. A.; Reichert, W. M.; Foley, M. P.; De Long, H. C.; Trulove, P. C. Process Variables That Control Natural Fiber Welding: Time, Temperature, and Amount of Ionic Liquid. *Cellulose* **2012**, *19*, 13−22.
(38) Ebner, G.; Schiehser, S.; Potthast, A.; Rosenau, T. Side Reaction of Cellulose with Common 1-Alkyl-3-Methylimidazolium-Based Ionic Liquids. *Tetrahedron Lett.* **2008**, *49*, 7322−7324.
(39) Proniewicz, L. M.; Paluszkiewicz, C.; Wesełucha-Birczyńska, A.; Majcherczyk, H.; Barański, A.; Konieczna, A. FT-IR and FT-Raman Study of Hydrothermally Degradated Cellulose. *J. Mol. Struct.* **2001**, *596*, 163−169.
(40) Watanabe, A.; Morita, S.; Kokot, S.; Matsubara, M.; Fukai, K.; Ozaki, Y. Drying Process of Microcrystalline Cellulose Studied by Attenuated Total Reflection IR Spectroscopy with Two-Dimensional Correlation Spectroscopy and Principal Component Analysis. *J. Mol. Struct.* **2006**, *799*, 102−110.
(41) Virtanen, T.; Maunu, S. L. NMR Spectroscopic Studies on Dissolution of Softwood Pulp with Enhanced Reactivity. *Cellulose* **2014**, *21*, 153−165.
(42) Larsson, P. T.; Hult, E.-L.; Wickholm, K.; Pettersson, E.; Iversen, T. CP/MAS 13C-NMR Spectroscopy Applied to Structure and Interaction Studies on Cellulose I. *Solid State Nucl. Magn. Reson.* **1999**, *15*, 31−40.
(43) Toomre, D.; Manstein, D. J. Lighting up the Cell Surface with Evanescent Wave Microscopy. *Trends Cell Biol.* **2001**, *11*, 298−303.
(44) Müller, U.; Rätzsch, M.; Schwanninger, M.; Steiner, M.; Zöbl, H. Yellowing and IR-Changes of Spruce Wood as Result of UV-Irradiation. *J. Photochem. Photobiol., B* **2003**, *69*, 97−105.

DOI: 10.1021/acssuschemeng.8b05059
ACS Sustainable Chem. Eng. 2019, 7, 3195−3202